NUMERICAL MODELS FOR ALUMINIUM HONEYCOMB SANDWICH STRUCTURES FRAGMENTATION

A. Abiti[(1)], C. Giacomuzzo[(1)], and L. Olivieri[(2)]

[(1)]*CISAS "G. Colombo", University of Padova, Via Venezia 15, 35131 Padova, Italy, Email: {alberto.abiti, cinzia.giacomuzzo}@unipd.it*

[(2)]*DII, University of Padova, Via Venezia 1, 35131 Padova, Italy, Email: lorenzo.olivieri@unipd.it*

ABSTRACT

The growing numbers of space debris pose a significant risk to man-made objects operating in Earth orbits, raising the probability of impacts that could lead up to the complete failure of the spacecraft. To better model the characteristics and behaviour of the fragments generated after in-orbit collisions, the simulation of these events plays a central role. In this context, the Collision Simulation Tool Solver (CSTS) is a semi-empirical software, capable of providing data on debris population generated after a collisional event.
This work aims to improve the material libraries of the software, including common-used aluminium honeycomb sandwich panels, and various approaches to simulate sandwich in CSTS fragmentation are explored. In this paper a preliminary model is shown that can obtain accurate data on the fragments produced from the simulation of four experimental cases. Further investigation is required to generalise this model for different collisional situations.

Keywords: Space debris; Honeycomb, Hypervelocity impact; Sandwich structures.

1. INTRODUCTION

The intensified use of near-Earth orbits in recent decades has led to a rapid increase in the space debris population [1]. In particular, density peaks can be observed in specific regions such as Low Earth Orbits (LEO) and, to a lesser extent, Geostationary Orbits (GEO) [2]. This issue has been well known since the beginning of space exploration era and various debris propagation models have been studied over the time [3]. This phenomenon poses a significant risk to human activities in Earth's orbital regions. Spacecrafts can be effectively protected from debris smaller than 1 mm through the use of dedicated shielding solutions [4]. For larger tracked debris, when the impact probability is deemed sufficiently high, collision avoidance manoeuvres must be performed when possible [5]. For scenarios, the ability to assess and understand fragmentation events and their consequences is essential [6, 7, 8]. In the first case, it allows the development of improved protection solutions by optimising shield geometries and materials in order to minimize the impact damage [9]. It also allows to evaluate how the critical components of the spacecraft would be affected depending on the collision conditions [10]. Moreover, in the second case, the construction of validated fragmentation models can help complete debris tracking data and can lead to a more accurate estimation of in-orbit impact probabilities.
Different strategies can be employed to develop such models. Analytic equations can provide fragments distributions in terms of size, shape, and velocity [11, 12]; however, they present limitations in representing all the parameters affecting orbital break-ups. On the other hand, hydrocode simulations provide highly detailed analyses of collision events but can be extremely computationally expensive [13]. Because of this, in recent years, the Space Debris Group of the University of Padova [14] has developed CSTS,

Proc. 9th European Conference on Space Debris, Bonn, Germany, 1–4 April 2025, published by the ESA Space Debris Office
Editors: S. Lemmens, T. Flohrer & F. Schmitz, (http://conference.sdo.esoc.esa.int, April 2025)

a semi-empirical software for impact modeling [15]. The software approximates the bodies involved in the impact using a coarse mesh of Macroscopic Elements (MEs), which serve as nodes of the structure, connected by structural links. Fragmentation, treated as a process with short time evolution where stresses exceed material strength, is simulated using semi-empirical models. Instead, the propagation of shock waves along the structure is modelled by tracking the momentum transferred to the MEs and the dissipated energy along the links, leading to the eventual failure of the structure. Compared to traditional hydrocodes, CSTS provides statistically accurate results in a considerably shorter CPU time. However, accurate tuning against experimental data is needed to provide realistic information about the fragments produced. Currently, the code has been tuned for commonly used materials such as aluminium and carbon reinforced polymers (CFRP), allowing the simulation of complex in-orbit fragmentation scenarios and obtaining statistically accurate debris distributions [16, 17]. However, further investigation is required to model all the materials and MEs present on board of satellites and rocket bodies.

This work focusses on expanding the material library of the software, including sandwich materials with aluminium honeycomb core. Sandwich panels represents a common-use solution in spacecraft due to their capacity to produce lightweight structures with high strength and high stiffness. Commonly associated with aluminium or CFRP external skins, honeycomb cores combine a high compression modulus with a low mass, making it possible to significantly space the external plates without excessively increasing the areal density. In addition, honeycomb cores increase the panel momentum of inertia and, as a consequence, the flexural strength compared to a single-plate structure of the same mass. [18].

This paper is organised as follows. In Section 2 an overview of the CSTS fragmentation algorithm is presented. Section 3 describes the approaches developed for modelling the fragmentation of these materials. Finally, Section 4 illustrates the results of the simulations and Section 5 discusses them.

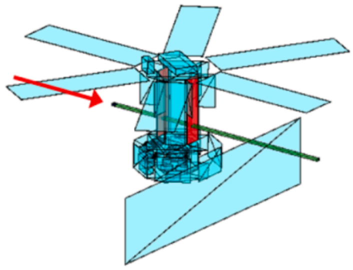

Figure 1: Discretization of a spacecraft using the Macroelements available in CSTS [20].

2. OVERVIEW ON CSTS

The software in development, CSTS, implements a hybrid approach to simulate hypervelocity impacts (HVI) [15]. The spacecraft structure is approximated using Macroscopic Elements (MEs), which are connected through different types of structural links; the MEs currently implemented in the code have a simple shape (e.g. plates, boxes, cylinders, spheres, etc.). An example of the discretization of the structure using MEs is shown in Fig. 1. The core idea behind the software is that the collisional event can be viewed as a combination of two phases with distinct time evolution: the first phase concerns the impact itself, which occurs within a very short time frame, typically on the order of milliseconds. The collision and subsequent formation of shock waves lead to the production of a cloud of fragments. Following this event, shock waves propagate through the structure, affecting its integrity. This second phase evolves over a longer period of time and affects the integrity of the structural links.

In order to incorporate this idea, CSTS operates through three main algorithms: the Breakup Algorithm, which describes the rapid fragmentation of the MEs, the Tracking Algorithm, which deals with the tracking of both fragments and MEs, and finally the Structural Response Algorithm. The last part of the code evaluates the eventual failure of the links, determining the large-scale response of the MEs network.

Focussing on the Breakup Algorithm, the process can be described as follows: when the impactor strikes the ME, a fragmentation volume is defined based on the energy of the collision and

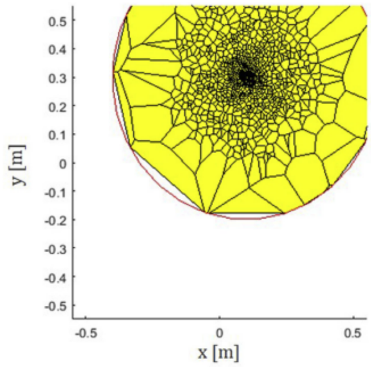

Figure 2: Voronoi fragmentation pattern applied to the fragmentation volume [15].

the material density. This volume is populated with a certain number of seeds, which are used to generate fragments, using a Voronoi pattern, as shown in Fig. 2.

The accuracy of this method strongly depends on the precision of the calibration with the experimental data and the capacity of tuning the seed generation in function of the impact parameters. For this reason, various strategies for generating seed distributions have been implemented in the code. For isotropic materials, such as metals and polymers, CSTS can use either a Gaussian distribution, which depends on two parameters, or a logarithmic spiral distribution, which instead depends on four parameters. These parameters were optimised for aluminium plates, using a genetic algorithm based on experimental data [15]. Furthermore, CSTS is capable of simulating fragmentation in CFRP materials using a dedicated algorithm [19]. In particular, this study aims to explore different approaches to modelling fragmentation also in sandwich materials, trying to obtain equivalent behaviours in terms of fragment production.

3. DEVELOPMENT OF ANALYSIS METHODS

When subjected to HVI impacts, honeycomb sandwich panels show a complex fragmentation behaviour. More specifically, the collision can be divided into three distinct phases: the initial impact of the projectile with the front plate, the interaction between the resulting debris cloud with the honeycomb cells, and the final impact of the modified cloud with the rear wall of the structure. As a result of honeycomb structure, fragments produced by the front plate face multiple impacts with the cell walls, which absorb their energy and reduce their size. However, the hexagonal cells limit the radial expansion of the debris cloud, as can be seen in Fig. 3. This phenomenon, known as channelling effect, has the negative result of concentrating the debris cloud within a smaller volume, reducing the impact area on the rear wall. As a consequence, the concentration of the damage reduces the shielding effectiveness of the sandwich structure compared to a Whipple structure, where the debris cloud is free to expand into the stand-off space [21]. In summary, an equivalent fragmentation model should account for both the filtering effect on fragments due to the multiple impacts with honeycomb cells and the increased fragmentation volume caused by the cloud concentration.

Furthermore, the impact angle significantly influences the fragmentation behaviour of the sandwich structure. The cell walls absorb the momentum of the debris cloud, reducing the energy transferred to the rear wall. The higher the collision angle, the higher the number of walls impacted, leading to a further reduction in the cloud energy [22].

With these premises, the first step was to identify some experimental tests reporting information about the characteristics of the fragments. Therefore, four experimental tests performed by CISAS research centre [23] were selected. These tests were performed using the CISAS Hypervelocity Impact Facility, able to accelerate projectile up to 100 mg at a maximum speed of 5.5 km/s using a two-stage Light-Gas-Gun (LGG) [24, 25, 26]. For each test, the impactors were aluminium spheres of 2.9 mm in diameter, launched in normal direction against three honeycomb sandwich panels; three samples were provided with aluminium skins, while the fourth one employed CFRP skins. The test parameters are listed in Tab. 1. From these experiments, the collision parameters to be implemented in the CSTS simulations were extracted.

Fig. 4 shows the experimental distribution of L_C. It can be observed that the resolution of the fragment dimension measurement is on the order of magnitude of 0.2 mm. CSTS is primarily used in satellite-scale simulations, where this level of detail is often unnecessary, and a resolution of 1

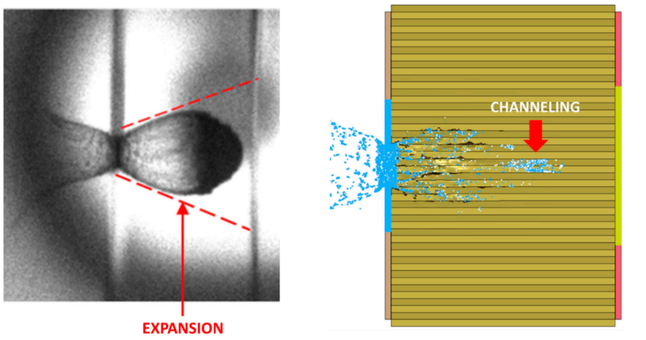

(a) (b)

Figure 3: Comparison of the cloud expansion in two configuration: high-speed photo of an experimental test on a Whipple shield (a) and a SPH simulation of a honeycomb sandwich (b). In honeycomb simulation is visible the contraction of the cloud caused by the channeling effect. [21]

Table 1: Experimental tests parameters.

Test ID	Skin material	Total thickness [mm]	Skin thickness [mm]	Total mass [g]	Projectile velocity [m/s]
Test 1	Al	25.4	1.1	28.846	4630
Test 2	Al	50.8	1.2	81.709	4710
Test 3	Al	25.4	1.1	30.422	3630
Test 4	CFRP	12.7	2.3	N.D	4800

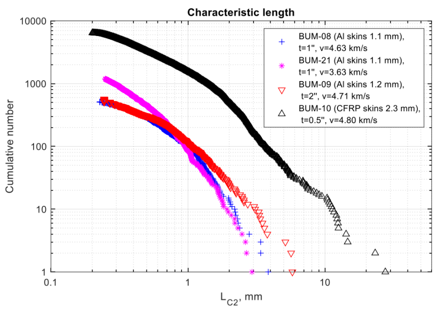

Figure 4: Experimental distribution of L_C [23].

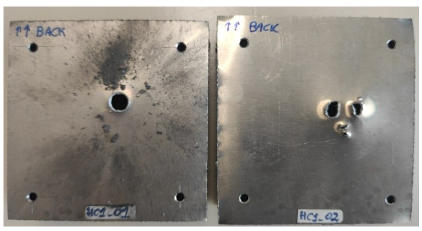

Figure 5: Comparison between test 1 (left) and test 3 (right) back side.

mm is typically set. However, this study aims to achieve the same resolution as the experimental tests.

Comparing the curves about test 1 and test 3 it can be observed that, even if in test 3 the target was hit by a projectile 1 km/s slower than test 1, it produced a significantly higher quantity of fragments. This can be explained by viewing Fig. 5, showing the back side of the sandwich structure of test 1 (on the left) and test 3 (on the right) after impact. In fact, test 1, presents a single circular crater, while test 3 presents multiple irregular holes. From this visual inspection and information about the fragment curves, it can be deduced that the test 3 projectile collided in correspondence with a honeycomb cell wall. This event led to a greater production of fragments compared to an impact happening in the centre of the honeycomb cell.

As a first step, a preliminary analysis was

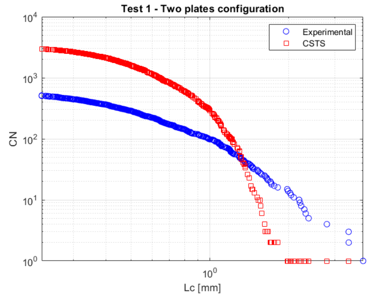

Figure 6: Comparison between experimental and simulated fragments characteristic length curves using the two-plates configuration.

performed evaluating the collision parameters in test 1 while ignoring the effect of the honeycomb core but considering only the skins. The structure was modelled in CSTS as two aluminium plates spaced by the width of the core. This approach allowed simulation to be performed using CSTS validated materials and provided an approximate estimation of the influence of the honeycomb on fragment production. The performance of each simulation against experimental data was evaluated by comparing the distribution of curves representing the cumulative number of fragments (CN) in function of their largest dimension (a) and their "bidimensional" characteristic length (L_C). The rationale behind this choice is that, as reported in [23], during the experimental procedure, the main dimensions of each fragment were measured using a 2D scanning procedure. For this reason, L_C is calculated using Eq. 1.

$$L_C = \frac{a+b}{2} \tag{1}$$

To ensure consistency when comparing the experimental curve with the simulation output, the three main dimensions of each fragment produced by CSTS were calculated, but only the two largest were considered in the L_C calculation. Fig. 6 shows the results of a preliminary simulation of test 1, using the "two plates" configuration. The CN-L_C curve is higher than the experimental one and has a different distribution, showing fewer fragment production in the range of 1.3 to 3.8 mm.

It is evident the necessity to introduce an approach to account both the channelling effect of the honeycomb and the filtering effect in fragment size as the collision angle varies. Two

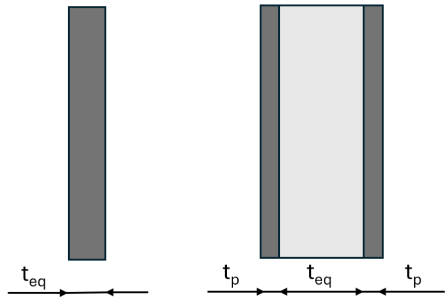

(a) (b)

Figure 7: Equivalent simulation approaches developed: single box (a) and triple box (b).

possible modelling approaches were evaluated, which are resumed in Fig. 7. The first possibility represents the sandwich structure as a single plate element with an equivalent fragmentation behaviour. The second approach, in contrast, models the external plates as a two-box configuration but introduces a middle-layer material calibrated to reproduce the effects of the aluminium honeycomb.

A choice was made to explore the single-box approach because this solution would allow reducing the computational time of the simulation. Therefore, collisions were modelled using a sphere ME to reproduce the projectile and a plate ME for the sandwich structure, both made of aluminium (or with the plate in CFRP in the case of test 4). The plates were designed using their real width and length and an equivalent thickness, calculated using Eq. 2 where m_{exp} is the measured mass of the sandwich structures, ρ_{Al} is the equivalent material density, and L_1 and L_2 are, respectively, the width and length of the plate.

$$t_{eq} = \frac{m_{exp}}{\rho_{Al} \cdot L_1 \cdot L_2} \tag{2}$$

The main issue in developing this approach is schematised in Fig. 8. An impact on a sandwich panel generates two craters, one on each wall: because of the contribution of the channelling effect, in the considered collision velocity ranges the crater on the rear wall is larger than the one that would be created if the honeycomb were not present. This difference in crater sizes caused simulations made with the algorithm already implemented for aluminium to be biased

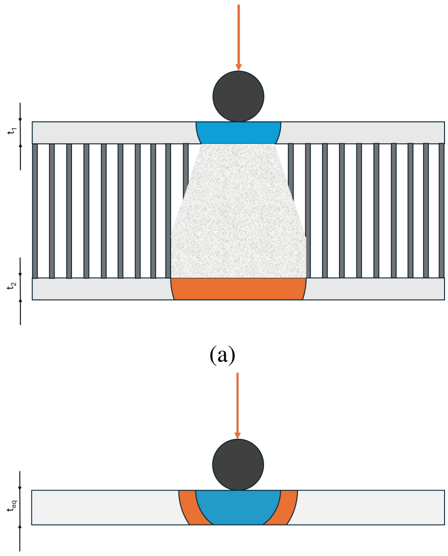

(a)

(b)

Figure 8: Scheme of an impact on sandwich panel (a) and CSTS equivalent strategy (b).

toward larger fragments, as shown in Fig. 9. To reproduce the sandwich behaviour using a single element, a property of CSTS breakup process was used: since the software reproduces a collision as a succession of multiple smaller impacts while both the projectile and the target fragment without changing their MEs geometry but only their mass, a control on the crater size during this process was introduced. In this way, during the initial steps, the crater computed by the software is enlarged through a factor named c_1. After a certain number of steps, controlled by the parameter c_{step}, the crater is no longer artificially widened but is narrowed using c_2. The last controlling parameter of the simulation is called c_{nseeds} and influences the number of fragments produced. In addition, seeds were generated using a Weibull distribution, instead of a Gaussian one, to better describe small fragments.

4. SIMULATION RESULTS

Starting from a first-try solution, the parameters of each simulation were optimised using a Genetic Algorithm (GA), running in Phyton and controlling CSTS in MATLAB. Multi-objective optimisation was performed to minimise the difference in the produced fragments Δ and maximise the value of the logarithmic determination coefficient, R^2_{log}, between the experimental and the simulated curve L_C. More specifically, GA was performed using 25 generations of 8 individuals, where the initial population was half formed by first-try solutions and half from randomly generated individuals. An example of the performance of the optimisation method is shown in Fig. 10 for test 2. Optimisation could be performed only for the tests on aluminium equivalent plates, since simulations on aluminium are faster than those on CFRP plates. For time calculation reasons, it was not possible to complete the optimisation process for Test 4. The results of the procedure for each test are reported in Tab. 2.

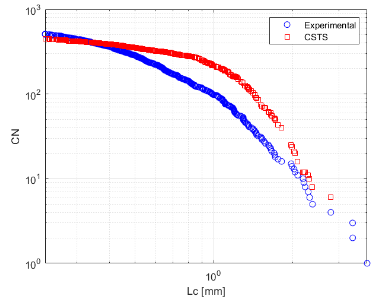

Figure 9: Simulation results using CSTS algorithm for aluminium.

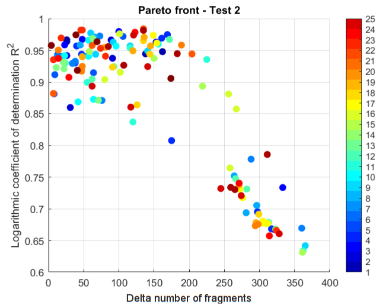

Figure 10: Multiobjective optimization on test 2. The procedure maximized R^2_{log} between experimental and simulated L_C curves and minimized the difference between produced fragments.

Finally, Fig. 11 shows the resulting a and L_C curves for each test with external aluminium plates. Through optimisation of the parameters,

Table 2: Optimized simulation parameters reported with the resulting R^2_{log} and Δ.

Test ID	c_1	c_2	c_{step}	c_{nseeds}	Δ	R^2_{log}
Test 1	0.5	0.27	30	0.39	2 (0.39%)	0.986
Test 2	0.45	0.26	30	0.31	49 (8.66%)	0.982
Test 3	0.35	0.3	20	0.01	49 (4.14%)	0.993
Test 4	0.45	0.3	30	1.5	27 (0.35%)	0.903

the simulated curves were obtained with R^2_{log} values always higher than 0.98 for the L_C curves and 0.97 for the a curves, combined with a small difference in the fragments produced. Regarding calculation time, the simulations requested, respectively, 12 minutes for Test 1, 7 minutes for Test 2 and 13 minutes for Test 3. As mentioned, for computational time reasons, it was not possible to complete GA for test 4: the optimisation of the CFRP algorithm is currently ongoing and the elaboration is significantly slower than the aluminium one. Moreover, CFRP-skin collision from test 4 produced roughly twenty times more fragments than test 1, despite similar impact conditions. For these reasons, the simulation, with this level of detail, took 14 hours, obtaining a L_C curve with R^2_{log} equal to 0.90 and a difference in the fragments produced of 0.35%. The results of test 4 are presented in Fig. 12.

Furthermore, Fig. 13 reports the curves resulting from the simulation that maintain the same parameters, but with a higher simulation resolution.

It should be mentioned that, in order to obtain curves with a good fit for 0.2 mm fragments, the CSTS resolution had to be set to 0.05 mm; this value is extremely low and cannot be used for complex fragment scenarios involving satellite-sized objects, due to the extremely high computational resources needed. In order to verify the performances of the sandwich panel algorithm for higher resolutions, this value was increased to 0.3 mm to obtain well-fitting curves up to 1 mm fragment dimensions. Even if the simulation parameters were not optimised for these resolutions, the resulting curves maintain a good fit to the experimental data.

5. DISCUSSION

The four simulations showed the possibility to obtain a good fit with the experimental data in terms of the fragments produced in a short calculation time. In particular, a similarity can be seen in the parameters for tests 1 and 2. However, this study represents only a preliminary step in the development of a general CSTS model for sandwich structures. In the paper a strategy was explored to obtain good fitting results controlling some parameters of the simulations. This method needs to be generalised by introducing more experimental data in a broader velocity range. Possible approaches would be to distinguish two different impact situations, letting the user decide whether the impact would occur on the corresponding wall of a honeycomb cell, as in test 2, or in the centre of it, as in tests 1 and 3, and differentiate it from the value of c_1 and c_2 or introduce a weighted random algorithm for multiple-collision scenarios. This is necessary because these situations present two very different cumulative number curves of fragments. Another step would be to study the repeatability in the value of c_{nseeds}, making it possible to control the number of fragments generated after the simulations. Finally, a consideration needs to be made about how the fragment distribution varies depending on the impact angle, since the available data in the literature refer only to normal collisions. This effect needs to be studied and introduced into the developed method as a modifier of the three introduced parameters. In order to obtain the necessary data, a test campaign is planned using CISAS' LGG. The tests will be carried out using aluminium and CFRP sandwich structures, varying impact parameters such as speed, direction, and projectile diameters to obtain more complete information.

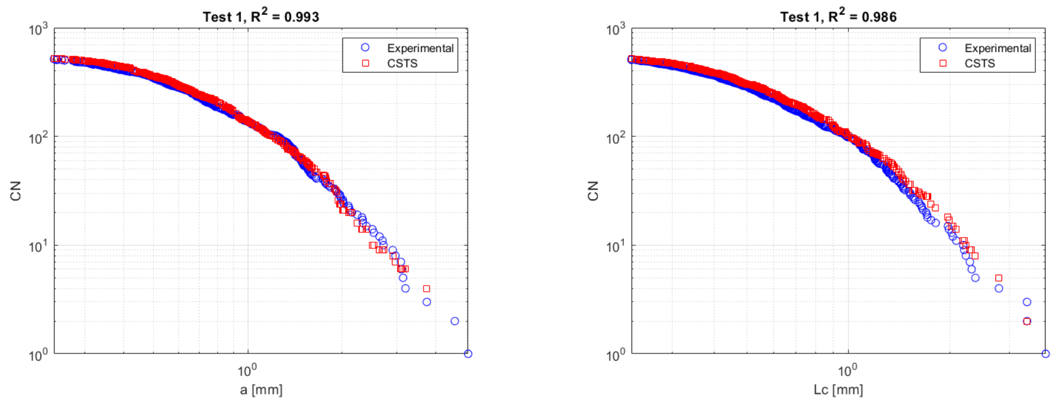

(a) Test 1

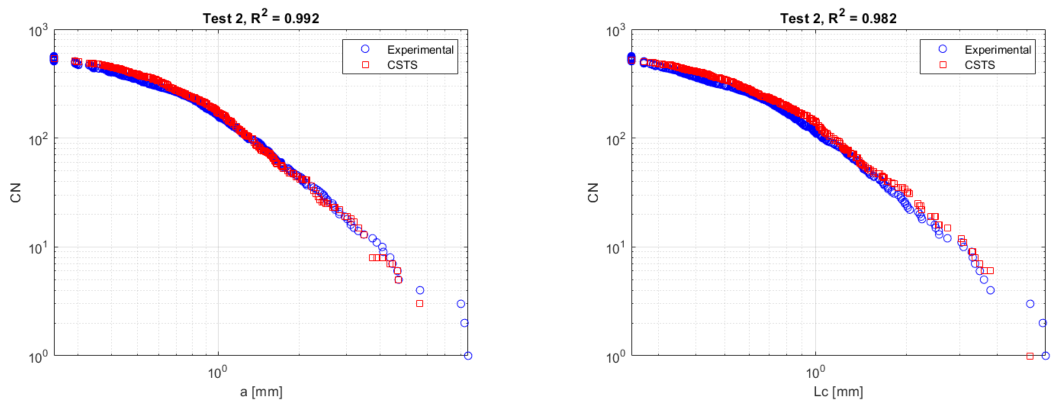

(b) Test 2

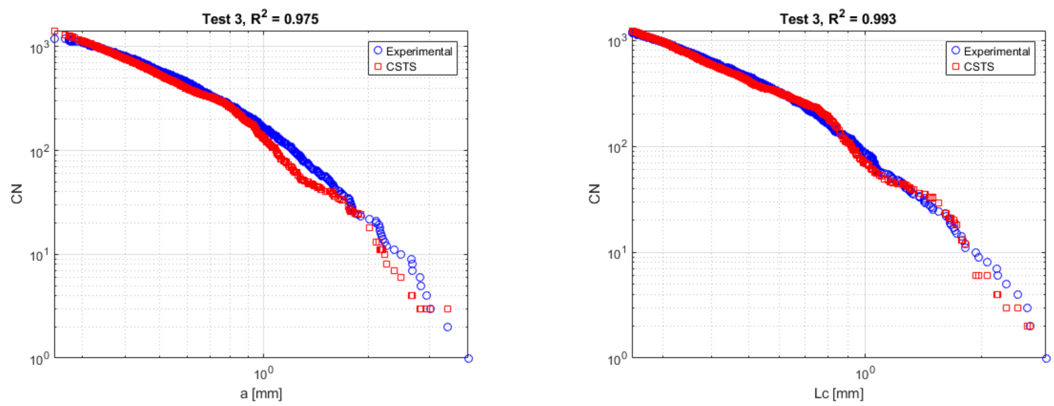

(c) Test 3

Figure 11: Comparison between L_C and a experimental and simulated curves for Test 1 (a), Test 2 (b) and Test 3 (c).

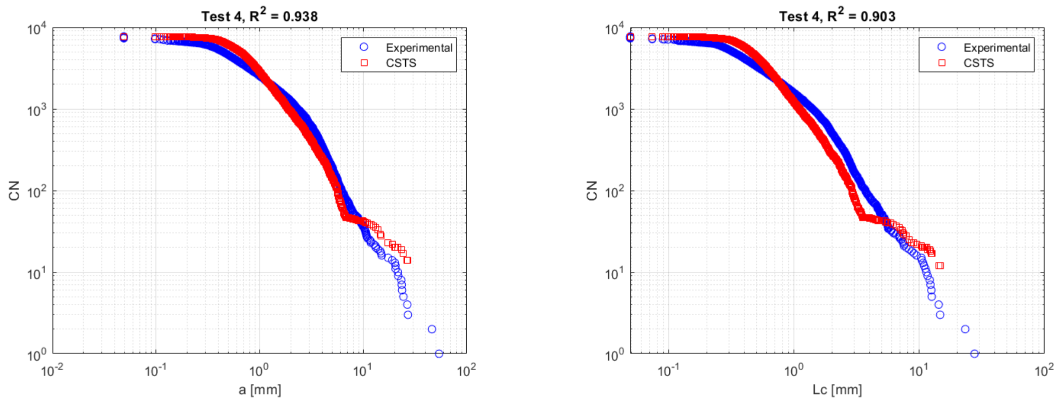

Figure 12: Comparison between L_C and a experimental and simulated curves for Test 4.

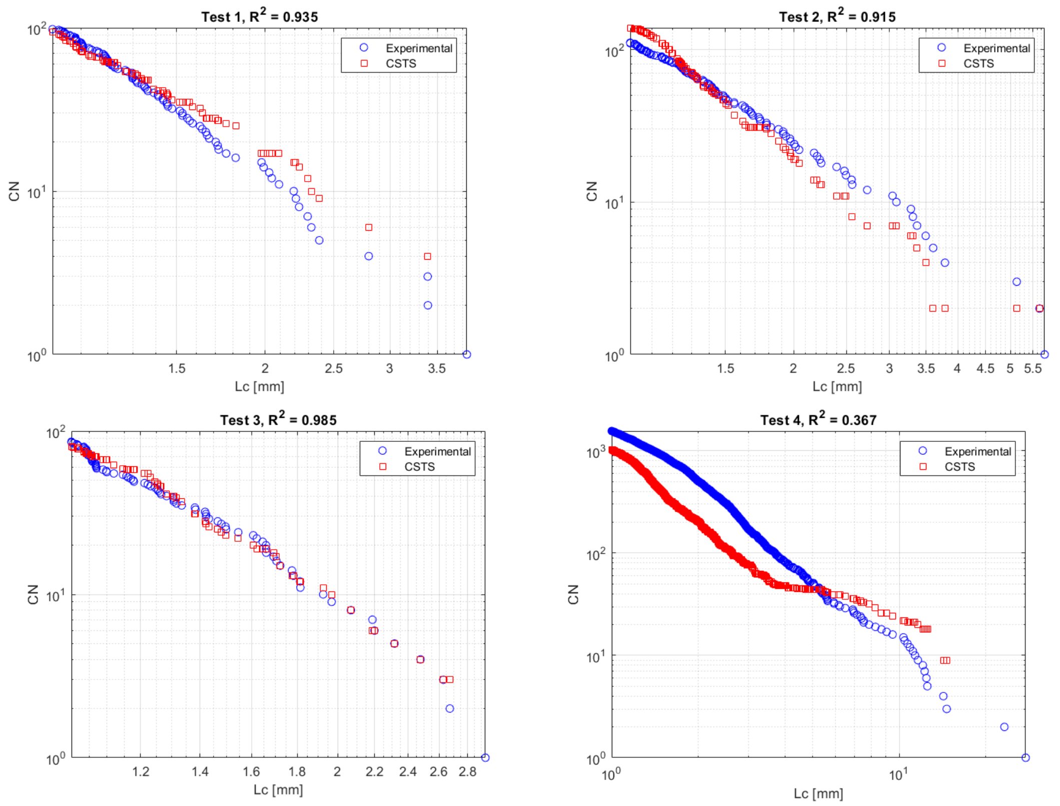

Figure 13: Experimental and simulated L_C curves with 1 mm fragments dimension resolution.

6. CONCLUSION

In this paper, a methodology to describe the fragmentation of sandwich panels with aluminium honeycomb in the CSTS software has been presented. After a preliminary study on the experimental data, four cases from internal tests were chosen to simulate in CSTS. After valuing different possible approaches, it was chosen to model the sandwich in the software as a single equivalent plate made of the same material of the external plates to minimise simulation CPU time. Standard CSTS models were not suitable to describe sandwich fragmentation, making it necessary to develop a different strategy based on three controlling parameters. Simulations were performed and the results were compared with the experimental curves of the characteristic length of the fragments.
The simulations described in this paper represent a preliminary result in the study: they demonstrated that CSTS is able to obtain equivalent results, in terms of produced fragments, using a single plate element, with a high level of significance; however, the small data sample employed in this work does not allow to generalise the obtained results to other impact configurations. More tests are therefore planned to study how varying those parameters may affect the simulations and how they can be adapted to generalise this strategy, including also the effect of the collision angle.

ACKNOWLEDGMENT

This work has been supported by the Italian Space Agency in the framework of the agreement n.2023-37-HH.0 “Attività tecnico-scientifiche di supporto a C-SSA/ISOC”.

REFERENCES

1. Anselmo, L., Rossi, A., Pardini, C. (1999). Updated results on the long-term evolution of the space debris environment. Advances in Space Research, 23(1), 201-211.
2. Schaub, H., Jasper, L. E., Anderson, P. V., McKnight, D. S. (2015). Cost and risk assessment for spacecraft operation decisions caused by the space debris environment. Acta Astronautica, 113, 66-79.
3. Kandel, D. B., Kessler, R. C., Margulies, R. Z. (1978). Antecedents of adolescent initiation into stages of drug use: A developmental analysis. Journal of Youth and adolescence, 7(1), 13-40.
4. Christiansen, E. L. (2003). Meteoroid/debris shielding (No. S-898). Houston: National Aeronautics and Space Administration, Lyndon B. Johnson Space Center.
5. Stoll, E., D’Souza, B., Virgili, B. B., Merz, K., Krag, H. (2013, March). Operational collision avoidance of small satellite missions. In 2013 IEEE Aerospace Conference (pp. 1-11). IEEE.
6. Johnson, N. L., Krisko, P. H., Liou, J. C., Anz-Meador, P. D. (2001). NASA’s new breakup model of EVOLVE 4.0. Advances in Space Research, 28(9), 1377-1384.
7. McKnight, D., Maher, R., Nagl, L. (1994). Fragmentation algorithms for strategic and theater targets (FASTT) empirical breakup model, Ver 3.0. DNA-TR-94-104, December.
8. Sorge, M. E., Mains, D. L. (2016). IMPACT fragmentation model developments. Acta Astronautica, 126, 40-46.
9. Buyuk, M. U. R. A. T., Kurtaran, H., Marzougui, D., Kan, C. D. (2008). Automated design of threats and shields under hypervelocity impacts by using successive optimization methodology. International Journal of Impact Engineering, 35(12), 1449-1458.
10. Schimmerohn, M., Matura, P., Watson, et al. (2021). Numerical investigation on the standard catastrophic breakup criteria. Acta Astronautica, 178, 265-271.
11. Schäfer, F. K. (2006). An engineering fragmentation model for the impact of spherical projectiles on thin metallic plates. International Journal of Impact Engineering, 33(1-12), 745-762.
12. Schonberg, W., Schäfer, F., Putzar, R. (2010). Hypervelocity impact response of honeycomb sandwich panels. Acta Astronautica, 66(3-4), 455-466.
13. Heberling, T., Terrones, G., Weseloh, W. (2018). Hydrocode simulations of a hypervelocity impact experiment over a range of velocities. International Journal of Impact Engineering, 122, 1-9.

14. Olivieri L., Giacomuzzo C., Lopresti S., Francesconi A. (2023) Research at the University of Padova in the Field of Space Debris Impacts against Satellites: An Overview of Activities in the Last 10 Years. Applied Sciences, 13(6), 3874

15. Francesconi, A., Giacomuzzo, C., Olivieri, L., et al. (2019). CST: A new semi-empirical tool for simulating spacecraft collisions in orbit. Acta Astronautica, 160, 195-205.

16. Olivieri, L., Giacomuzzo, C., Francesconi, A. (2024) Numerical simulation of COSMOS 2499 fragmentation. CEAS Space J.

17. Olivieri L., Giacomuzzo C., Duran-Jimenez C., Francesconi A., Colombo C. (2021) Fragments distribution prediction for ENVISAT catastrophic fragmentation. 8th European Conference on Space Debris, 20 April 2021 - 23 April 2021, Darmstadt, Germany

18. Shifa, M., Tariq, F., Chandio, A. D. (2021). Mechanical and electrical properties of hybrid honeycomb sandwich structure for spacecraft structural applications. Journal of Sandwich Structures & Materials, 23(1), 222-240.

19. Lopresti S., Abiti A., Giacomuzzo C., Olivieri L., Polli E. M., Francesconi A. (2024) A numerical model for CFRP fragmentation under hypervelocity impacts. IAC 2024, Milano, 14-18 October 2024

20. Francesconi, A., Giacomuzzo, C., Olivieri, L., et al. (2022). Numerical simulations of hypervelocity collisions scenarios against a large satellite. International Journal of Impact Engineering, 162, 104130.

21. Carriere, R., Cherniaev, A. (2021). Hypervelocity impacts on satellite sandwich structures—A review of experimental findings and predictive models. Applied Mechanics, 2(1), 25-45.

22. Kang, P., Youn, S. K., Lim, J. H. (2013). Modification of the critical projectile diameter of honeycomb sandwich panel considering the channeling effect in hypervelocity impact. Aerospace Science and Technology, 29(1), 413-425.

23. Olivieri, L., Giacomuzzo, C., Francesconi, A. (2022). Impact fragments from honeycomb sandwich panels. In Proceedings of the International Astronautical Congress, IAC (Vol. 2022). International Astronautical Federation, IAF.

24. Angrilli, F., Pavarin, D., De Cecco, M., Francesconi, A. (2003). Impact facility based upon high frequency two-stage light-gas gun. Acta Astronautica, 53(3), 185-189.

25. Pavarin, D., Francesconi, A. (2003). Improvement of the CISAS high-shot-frequency light-gas gun. International journal of impact engineering, 29, 549-562.

26. Francesconi, A., Pavarin, D., Bettella, A., Angrilli, F. (2008). A special design condition to increase the performance of two-stage light-gas guns. International Journal of Impact Engineering, 35(12), 1510-1515.